J Solid State Electrochem (2003) 7: 232–238
DOI 10.1007/s10008-002-0309-0

ORIGINAL PAPER

S.A. Suthanthiraraj · R. Mala

Synthesis and characterization of ambient temperature superionic solids in the composite system CuI–Ag_2O–TeO_2

Received: 25 March 2002 / Accepted: 22 July 2002 / Published online: 26 September 2002

Abstract The present work deals with the composite system $(CuI)_x$–$(Ag_2O–TeO_2)_{100-x}$, where $x = 30$, 35, 40, 45, 50, 55, 60, 65, 70 and 75 mol%, respectively, synthesized by a solid-state reaction route. Powder specimens were analysed using differential scanning calorimetry, X-ray diffraction and Fourier transform infrared techniques. These studies have revealed the formation of Cu_3TeO_6, AgI and/or other phases. The ambient temperature electrical conductivities obtained for the samples using a complex impedance method were found to lie in the range 10^{-6}–10^{-4} Scm^{-1}, with low activation energies, thus indicating their superionic nature. The typical composition 35CuI–32.5Ag_2O–32.5TeO_2 was identified as the best conducting one, having an electrical conductivity of 6×10^{-4} Scm^{-1} at 296 K and an activation energy of 0.23 eV. Ion transport number measurements carried out using Wagner's polarization technique as well as by an electromotive force method suggested that silver ions were responsible for the observed transport features of the composite system.

Keywords Differential scanning calorimetry · X-ray diffraction · Fourier transform infrared technique · Complex impedance analysis · Ion transport number

Introduction

The most significant development witnessed over the last few decades has been the spread of electrochemical concepts into very different areas of research and development. On the basis of research by many electrochemists, physicists and materials researchers solid-state ionics involving superionic conductors is now used in a wide range of applications, such as solid-state batteries, fuel cells, gas sensors, pacemakers, electrochemical display devices, etc. [1, 2, 3, 4]. Superionic conductors or solid electrolytes are usually characterized by their appreciably high ionic conductivity and negligible electronic conductivity values [5]. Among the various superionic conductors investigated to date, silver-based materials are found to exhibit high ionic conductivities at room temperature. As a result of a higher degree of covalency leading to fewer surrounding anions and large polarizability, Ag^+ ions tend to possess interesting superionic properties. The presence of large and highly polarizable I^- ions in the form of the dopant salt in a superionic system appears to widen the diffusion pathway of the mobile ions, namely Ag^+ ions. A large number of binary, pseudo-binary and ternary mixed systems were reported to exhibit silver ion transport at ambient conditions [6]. Earlier, Minami [7] introduced AgI as a dopant salt into several oxysalt matrices, such as Ag_2O–MoO_3, Ag_2O–CrO_3 and Ag_2O–P_2O_5 and observed high ionic conductivities at room temperature. Similarly, Rossignol et al. [8] also employed AgI as the dopant in the case of a Ag_2O–TeO_2 matrix and reported silver ion transport. In our laboratory, many silver ion conducting superionic materials were already developed by the combination of CuI with silver oxysalts such as Ag_2O–PbO_2 [9], Ag_2O–V_2O_5 [10], Ag_2MoO_4 [11], Ag_2CrO_4 [12] and $Ag_4P_2O_7$ [13]. More recently, several mixed systems, like $Cu_{1-x}Ag_xI$–Ag_2O–B_2O_3 [14] $Cu_{1-x}Ag_xI$–Ag_2O–MoO_3 [15] and $Cu_{1-x}Ag_xI$–Ag_2O–SeO_2 [16] have also been examined during the course of our investigations concerning silver ion transport. Essentially, the present work involves detailed structural, thermal and electrical transport studies on the mixed system CuI–Ag_2O–TeO_2, in which CuI is employed as the dopant salt.

S.A. Suthanthiraraj (✉)
Department of Energy, School of Energy and Material Sciences, University of Madras, Guindy Campus, Chennai 600 025, India
E-mail: saustin@tatanova.com
Tel.: +91-44-2301576
Fax: +91-044-2350305

R. Mala
Department of Physics,
Bharathi Women's College, Chennai 600 108, India

Experimental

Sample preparation

Analar grade chemicals of CuI, Ag_2O and TeO_2 were used as raw materials for the preparation of various compositions of the new ternary system CuI–Ag_2O–TeO_2. Stoichiometric compositions of $(CuI)_x$–$(Ag_2O–TeO_2)_{100-x}$, where $x = 30$, 35, 40, 45, 50, 55, 60, 65, 70 and 75 mol%, were prepared by annealing appropriate amounts of the starting materials in ceramic boats in air at 773 K for 5 h and rapidly quenching the molten mixture in liquid nitrogen. Interestingly, the product was found to be grey, which may be attributed to the presence of aggregates of metallic silver within the specimen. The most probable reason for the formation of silver may be visualized in terms of the decomposition of Ag_2O at atmospheric conditions at 423 K. In other words, when CuI, Ag_2O and TeO_2 were annealed at 773 K in air in ceramic boats, a small fraction of Ag^+ ions released from Ag_2O could probably be reduced to metallic silver owing to the partial covalency of the bonding within the crystal structure of Ag_2O. Thus, the formation of elemental silver in traces during the process of preparation of the various samples was not avoidable.

Differential scanning calorimetry

The thermal events were recorded in the temperature range 343–573 K using a PerkinElmer model DSC7 differential scanning calorimeter at a heating rate of 20°min^{-1} with platinum as the reference material and aluminium sample containers.

Powder X-ray diffraction

X-ray diffraction (XRD) measurements were carried out on powdered samples at room temperature using a Philips X′ Pert-MPD X-ray generator unit with Cu Kα radiation (1.5406 Å) at various glancing angles (2θ) between 80° and 20°.

Fourier transform infrared analysis

Fourier transform infrared (FTIR) spectra were recorded for the various samples of the system in the wave number region 400–1500 cm^{-1} by the KBr pellet method at room temperature, using a PerkinElmer Paragon 500 model spectrometer.

Complex impedance analysis

The solid samples were ground and pressed together with silver electrodes on both sides under a pelletizing pressure of 5 toncm^{-2} to make circular pellets of 8-mm diameter. The electrodes were made up of metallic silver powder and sample mixed in the weight ratio 2:1. The complex impedance measurements were carried out in air using a Hewlett-Packard model HP4284A precision LCR meter in the frequency range 20 Hz–1 MHz and over the temperature range 296–403 K. The values of the bulk resistance, R_b, obtained from the complex impedance plots were used to calculate the electrical conductivity. σ, of the various compositions of the CuI–Ag_2O–TeO_2 system as outlined in the following.

Since superionic conductors or solid electrolytes are mostly studied in the form of polycrystalline samples, grain-boundary impedances would influence the evaluation of their bulk conductivity values. In this context, complex plane diagrams may be employed for the extraction of bulk conductivity values and separation of electrode and grain-boundary components from the experimental data. However, in the case of practical solid electrolyte systems, the analysis of bulk properties and the separation of grain-boundary as well as electrode–electrolyte interfacial effects are not simple and the selection of an appropriate equivalent circuit is also difficult owing to inhomogenities in the bulk, which make the observed bulk impedance frequency-dependent [17, 18].

A schematic representation of a polycrystalline superionic solid sandwiched between two nonblocking (i.e., reversible) electrodes together with the relevant equivalent circuit and impedance plot are shown in Fig. 1. According to Macdonald [19], such a complex impedance plot drawn over a range of frequencies would consist of three arcs, including a high-frequency one which is associated with the bulk conductivity (due to electrolytic resistance, R_b) shunted by the geometric capacitance, C_g, (capacitative coupling between the electrodes), while the arc of intermediate frequencies shows the influence of the geometric capacity and the impedance of double layer capacitance, C_{dl}, associated with the charge-transfer (charging and discharging at the electrode/electrolyte interface) processes. On the other hand, the low-frequency arc is usually inclined at an angle of about 45° to the real axis and it is specifically attributed to Z_d, the impedance due to the diffusion process arising from the presence of a concentration gradient within the electrolyte. In the case of real solid electrolytes, all these three arcs may not be present or only a part of the arc could be identified. Generally, the behaviour of the bulk electrolyte and that of the interfacial impedance are quite different from each other. However, in most of the systems, there is a distinct minimum in Z'' between the two regions as indicated in Fig. 1 and the value of Z' at this minimum of Z'' is the best estimate for the overall bulk resistance (including the constriction resistance, R_c, between the grains). Extrapolation of the impedance to higher frequencies in the interface dispersion region or to lower frequencies in the bulk dispersion region is also known to provide another way of determination of the bulk resistance from the complex plane impedance plots [20, 21, 22].

During the present investigation, the frequency response of a variety of compositions of the CuI–Ag_2O–TeO_2 system was measured in terms of the real (Z') and imaginary (Z'') parts of the

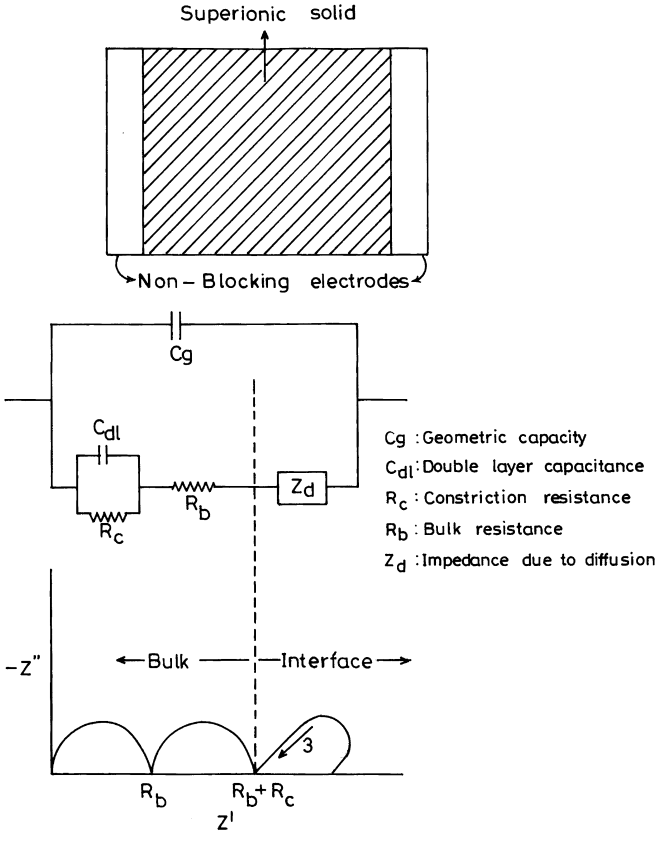

Fig. 1 Schematic diagram of a superionic solid sandwiched between a pair of nonblocking electrodes along with the corresponding equivalent circuit and impedance plot

complex impedance, Z^*, at different temperatures. The point of intersection of the impedance plots on the real axis in the high-frequency region was taken as the bulk resistance of the sample.

Ion transport number measurements

Wagner's polarization method

The ion transport number measurements were carried out on all the samples using Wagner's polarization method [23, 24]. For this purpose, a cylindrical pellet of the sample was sandwiched between an ion-blocking electrode (graphite) and a nonblocking electrode (silver). This pellet was placed between two silver plates and a constant direct current potential of 0.5 V was applied across the sample, keeping the silver electrode at the negative potential. The variation of the current in the circuit was noted as a function of time for about 7 h till the current became constant, indicating the fully depleted condition of the blocking electrode. This constant current would correspond to the electronic current. The average ion transport number, $\bar{t}_{ion}$, of the sample was determined by using the relation

$$\bar{t}_{ion} = I_{ion}/I_t, \quad (1)$$

where I_{ion} is the current due to the mobile ions and I_t is the total current due to all the mobile species,

$$\text{i.e., } I_t = I_{ion} + I_{e,h}, \quad (2)$$

where $I_{e,h}$ is the current due to electrons and holes.

Silver ion transport number measurements

The electromotive force (EMF) method was employed for the estimation of the ion transport number in these new materials. A galvanic cell was fabricated with a configuration

$$(-)\text{Ag} + \text{sample}/\text{sample}/I_2(+),$$

where a powder mixture of metallic silver powder and the sample in the weight ratio 2:1 were used as anode. The cell components were cascaded and pressed together at a pelletizing pressure of 5 toncm^{-2} to fabricate the galvanic cell. The values of the open circuit voltage of the cells were measured and compared with the thermodynamic value of 687 mV at room temperature reported for the typical solid-state electrochemical cell (–)Ag/AgI/I_2(+) having the following overall cell reaction:

$$2\text{Ag} + \text{I}_2 \rightarrow 2\text{AgI} \quad (3)$$

As this cell reaction may also be involved in the cells considered during the present investigation, it is quite relevant to use the same thermodynamic value of 687 mV for the present case as well [25]. The silver ion transport number which indicated the extent of silver ion contribution to the total electrical conductivity was determined for the various compositions in the CuI–Ag_2O–TeO_2 ternary system.

Results and discussion

Differential scanning calorimetricanalysis

The differential scanning calorimetry results obtained for ten compositions of the mixed system $(CuI)_x$–$(Ag_2O–TeO_2)_{100-x}$, where $x = 30$, 35, 40, 45, 50, 55, 60, 65, 70 and 75 mol%, are shown in Table 1. Endothermic peaks were observed at 423, 424, 423, 423, 423, 423, 423, 424, 422 and 423 K, respectively. These transition temperatures at which the endothermic peaks occur for the synthesized samples are comparable to the characteristic $\beta \rightarrow \alpha$ phase-transition temperature of pure AgI which is about 420 K. Therefore, this study has clearly indicated the formation of AgI in all the synthesized samples.

Table 1 Differential scanning calorimetry (*DSC*) results obtained for the mixed system $(CuI)_x$–$(Ag_2O–TeO_2)_{100-x}$, where $30 \le x \le 75$

Composition CuI–Ag_2O–TeO_2 (mol%)	DSC endothermic peak (K)
30:35:35	423
35:32.5:32.5	424
40:30:30	423
45:27.5:27.5	423
50:25:25	423
55:22.5:22.5	423
60:20:20	423
65:17.5:17.5	424
70:15:15	422
75:12.5:12.5	423

XRD analysis

The powder XRD patterns obtained at room temperature for ten different compositions of the ternary system $(CuI)_x$–$(Ag_2O–TeO_2)_{100-x}$, where $x = 30$, 35, 40, 45, 50, 55, 60, 65, 70 and 75 mol%, respectively, are shown in Fig. 2. The appearance of XRD peaks at around $2\theta = 23$, 32.5, 38, 42, 44, 47, 49, 54, 56, 58, 60, 62, 63, 65, 66, 68, 71 and 74° in all the patterns tends to show the presence of Cu_3TeO_6 in these samples. Since more intense peaks corresponding to Cu_3TeO_6 are also observed in all the compositions, Cu_3TeO_6 may be considered as the major content in these samples. The XRD peaks observed at around $2\theta = 24$, 39 and 46° and at around 35.5 and 38.7° indicate the formation of AgI and CuO, respectively, in all these samples. Furthermore, the XRD peaks occurring around $2\theta = 26$ and 30° tend to reveal the presence of Te_2O_5 in the case of compositions corresponding to $x = 30$, 45, 50, 55 and 65 mol%, while those appearing at 38° in the case of $x = 30$ and 35 mol% suggest the presence of Ag in these samples. The presence of metallic silver may be attributed to the most probable decomposition of Ag_2O during the annealing of the starting materials as described earlier. The formation of Cu_3TeO_6 and CuO may be explained as follows.

In the molten mixture containing CuI, Ag_2O and TeO_2, Cu^+ ion is a highly reducing species which may be oxidized to Cu^{2+} ion, thus forming CuO:

$$16\text{CuI} + 8\text{Ag}_2\text{O} + 4\text{O}_2 \rightarrow 16\text{CuO} + 16\text{AgI} \quad (4)$$

Simultaneously, the Te^{4+} ion in TeO_2 may be oxidized to Te^{5+} in order to form Te_2O_5, whereas some of the Te^{5+} ions in Te_2O_5 may be further oxidized to Te^{6+} ions, thus forming an intermediate product, TeO_3, in accordance with the following reactions:

$$8\text{TeO}_2 + 2\text{O}_2 \rightarrow 4\text{Te}_2\text{O}_5, \quad (5)$$

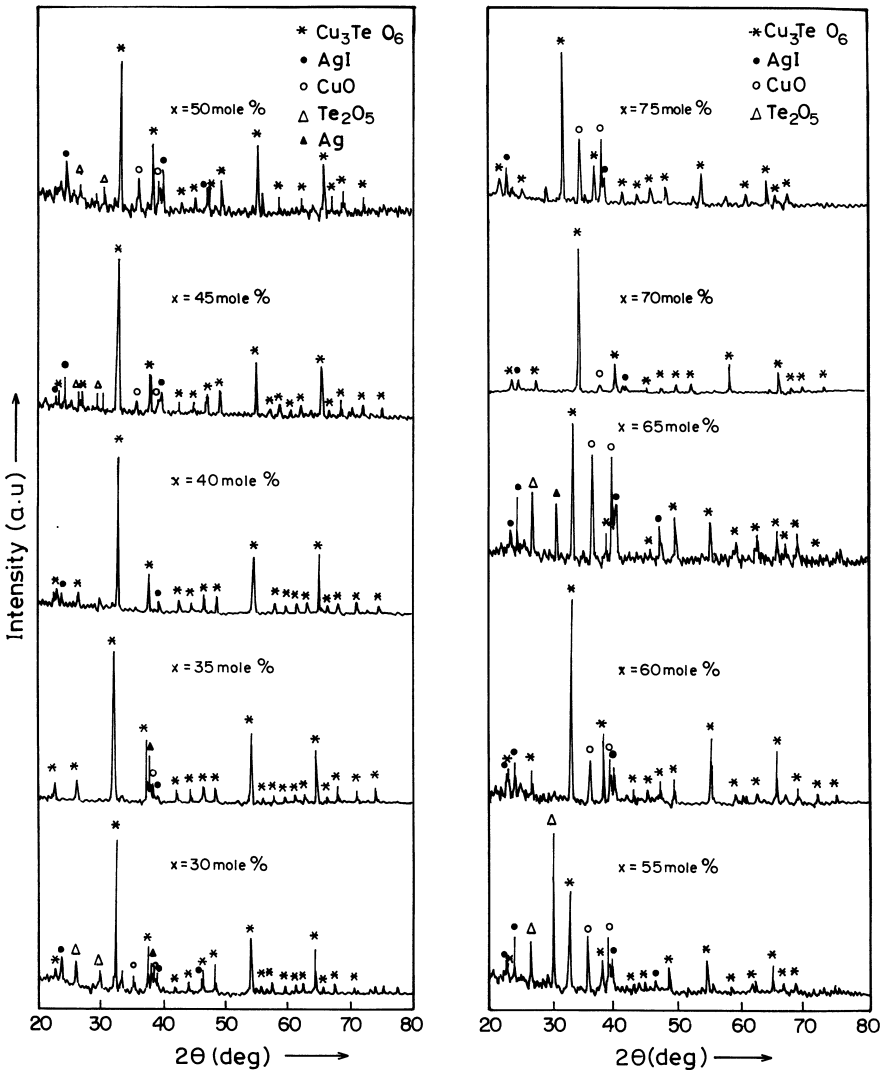

Fig. 2 X-ray diffraction patterns for the system $(CuI)_x$–$(Ag_2O–TeO_2)_{100-x}$, where $x = 30$, 35, 40, 45, 50, 55, 60, 65, 70 and 75 mol%, respectively

$$2Te_2O_5 + O_2 \rightarrow 4TeO_3. \quad (6)$$

Both these intermediate products, namely TeO_3 and CuO, may combine to form the final reaction product, i.e., Cu_3TeO_6 complex, according to the solid-state reaction

$$12CuO + 4TeO_3 \rightarrow 4Cu_3TeO_6. \quad (7)$$

Therefore, the most probable solid-state reaction during the melting process performed in air may be expressed as follows:

$$8TeO_2 + 16CuI + 8Ag_2O + 7O_2 \rightarrow 4Cu_3TeO_6 + 2Te_2O_5 + 16AgI + 4CuO. \quad (8)$$

From the XRD results it has also been realized that the synthesized samples are multiphase in nature with Cu_3TeO_6 and AgI and/or other phases as their possible constituents. It is evident from the previous discussion that the XRD results are in good agreement with the proposed reaction mechanism involving CuI, Ag_2O and TeO_2 as starting materials.

FTIR analysis

The FTIR spectral patterns obtained for five typical compositions of the ternary system $(CuI)_x$–$(Ag_2O–TeO_2)_{100-x}$, where $x = 30$, 45, 55, 65 and 75 mol%, respectively, are shown in Fig. 3. This figure clearly indicates the occurrence of absorption bands around 700 and 640 cm^{-1} in all the samples. These absorption bands may be attributed to the ν_1 and ν_3 vibrational modes of TeO_6 groups [26]. Further, the absorption bands observed around 500 and 410 cm^{-1} tend to reveal the presence of CuO groups [27]. These results are found to be consistent with the XRD results discussed earlier.

Electrical conductivity data

Typical complex impedance plots obtained for the composition $35CuI–32.5Ag_2O–32.5TeO_2$ at four different temperatures, namely 296, 308, 321 and 336 K, are shown in Fig. 4. These plots are found to exhibit a

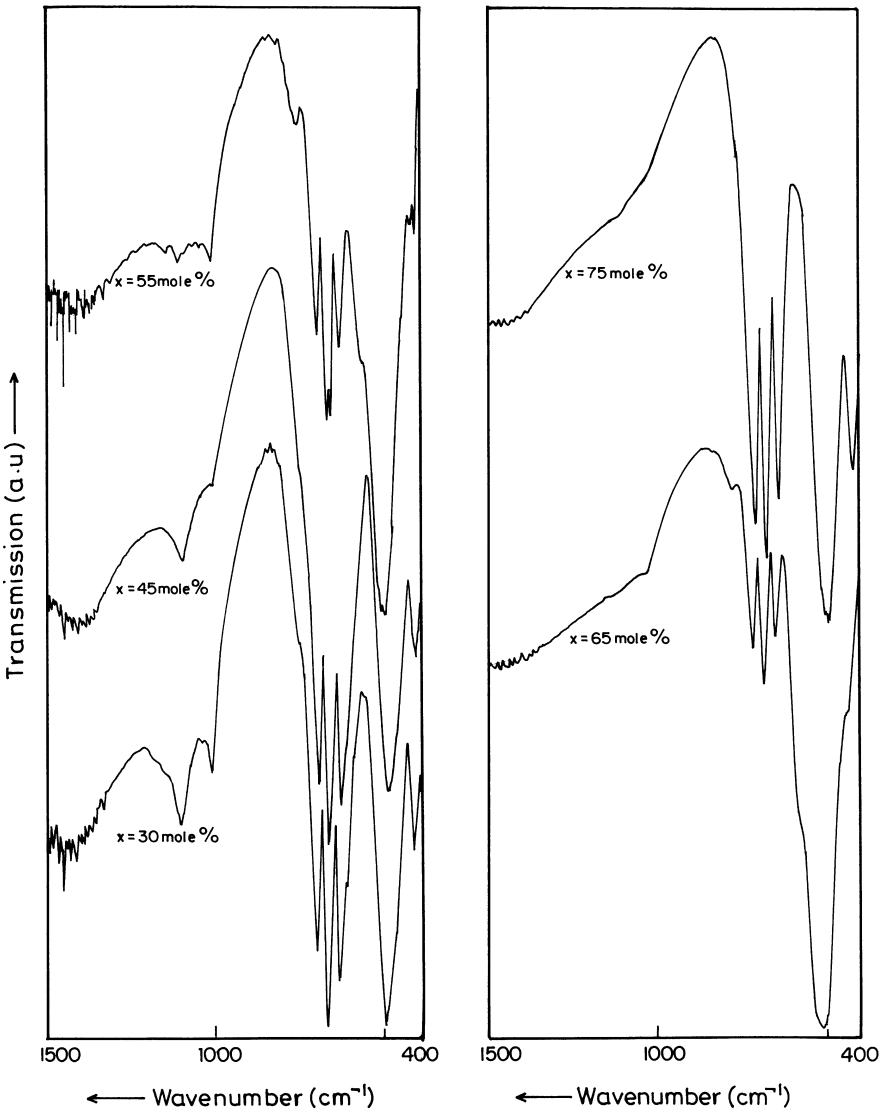

Fig. 3 Fourier transform IR spectra for the system $(CuI)_x$–$(Ag_2O–TeO_2)_{100-x}$, where $x = 30$, 45, 55, 65 and 75 mol%, respectively

portion of a semicircle whose intersection on the real axis corresponds to the bulk resistance at the appropriate temperature. These bulk resistance values are found to decrease as the temperature increases, thus revealing the ionic nature of these samples. Moreover, from the values of the bulk resistance evaluated from the impedance plots, electrical conductivity, σ, values were estimated using the general relationship

$$\sigma = t/(AR_b), \tag{9}$$

where t denotes the thickness of the sample pellet and A its area of cross-section.

The variation of $\log\sigma_T$ is shown in Fig. 5 as a function of the reciprocal of absolute temperature for the various compositions in the mixed system $(CuI)_x$–$(Ag_2O–TeO_2)_{100-x}$, where $x = 30$, 35, 40, 45, 50, 55, 60, 65, 70 and 75 mol%, respectively, in the temperature range 296–403 K. From Fig. 5 it is evident that in the temperature range of investigation, all the compositions obey the Arrhenius relationship

$$\sigma_T = \sigma_0 \exp(-E_a/kT), \tag{10}$$

where σ_0 is the preexponential factor, E_a the activation energy for the conduction process and k the Boltzmann constant. Usually, the activation energy for the conduction phenomenon represents the minimum energy required by the conducting species, namely ions, for migrating from one lattice site to another within the solid. The values of the activation energy were also evaluated from the slopes of these plots drawn by the least-squares method and were found to be less than 0.48 eV. This feature tends to indicate the superionic nature of the samples prepared. The room temperature electrical conductivity, $\sigma_{296\,K}$, and the activation energy data obtained for the various compositions of the present system are displayed in Table 2.

From Table 2 it is clear that the composition having the highest electrical conductivity of 6×10^{-4} Scm^{-1} at 296 K has been identified as $35CuI–32.5Ag_2O–32.5TeO_2$

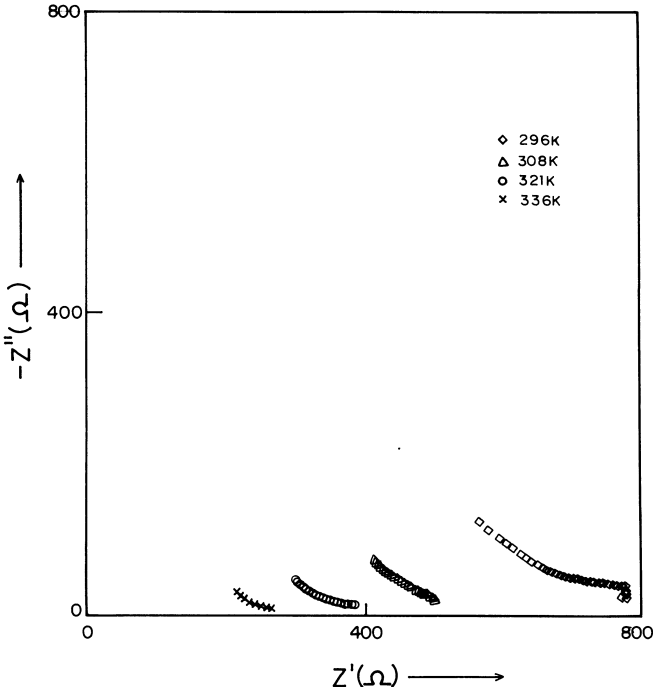

Fig. 4 Complex impedance plots for the composition 35 mol% CuI–32.5 mol% Ag_2O–32.5 mol% TeO_2 at various temperatures

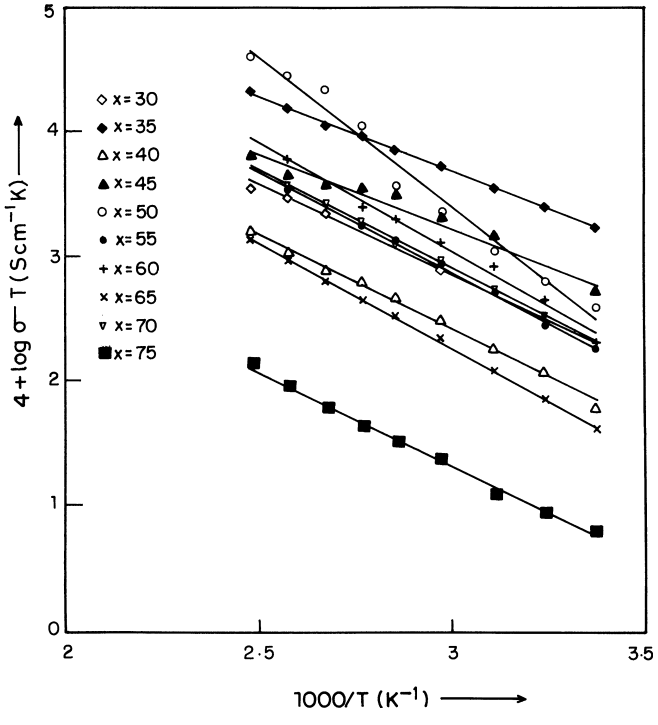

Fig. 5 Variation of $\log(\sigma T)$ with inverse of absolute temperature for ten different samples of the system $(CuI)_x$–$(Ag_2O$–$TeO_2)_{100-x}$ having $x = 30$, 35, 40, 45, 50, 55, 60, 65, 70 and 75 mol%, respectively

in the case of the CuI–Ag_2O–TeO_2 composite system in the solid state, thus indicating its superionic nature in ambient conditions.

Table 2 Room temperature electrical conductivity and activation energy data obtained for the mixed system $(CuI)_x$–$(Ag_2O$–$TeO_2)_{100-x}$, where $30 \le x \le 75$

Composition CuI–Ag_2O–TeO_2 (mol%)	Room temperature electrical conductivity, (Scm^{-1})	Activation energy (eV)
30:35:35	5.8×10^{-5}	0.29
35:32.5:32.5	6×10^{-4}	0.23
40:30:30	2×10^{-5}	0.3
45:27.5:27.5	1.8×10^{-4}	0.23
50:25:25	1.4×10^{-4}	0.48
55:22.5:22.5	6.1×10^{-5}	0.32
60:20:20	6.7×10^{-5}	0.34
65:17.5:17.5	1.4×10^{-5}	0.33
70:15:15	7×10^{-5}	0.31
75:12.5:12.5	2.2×10^{-6}	0.3

Table 3 Observed ion transport number data for the ternary system $(CuI)_x$–$(Ag_2O$–$TeO_2)_{100-x}$, where $30 \le x \le 75$

Composition CuI–Ag_2O–TeO_2 (mol%)	Ion transport number (Wagner's method)	Silver ion transport number (electromotive force method)
30:35:35	0.97	0.96
35: 32.5:32.5	0.99	0.98
40:30:30	0.96	0.97
45:27.5:27.5	0.97	0.98
50:25:25	0.97	0.97
55:22.5:22.5	0.97	0.97
60:20:20	0.96	0.98
65:17.5:17.5	0.95	0.96
70:15:15	0.97	0.96
75:12.5:12.5	0.96	0.95

Ion transport number data

The values of the ion transport number, $\bar{t}_{ion}$, evaluated by Wagner's direct current polarization method as well as the silver ion transport number, $\bar{t}_{Ag^+}$, data obtained by the EMF method for the various compositions in the system are given in Table 3. From Table 3 it is obvious that the $\bar{t}_{ion}$ values evaluated by Wagner's method are 0.95 or greater for all ten different compositions of the present CuI–Ag_2O–TeO_2 system. This reveals that the mobile species in this system are ionic in nature and that the electronic contribution to the total electrical conductivity would be negligible as compared to the ionic conductivity of these new compositions.

Furthermore, from Table 3 it is also evident that the $\bar{t}_{Ag^+}$ values obtained by the EMF method are 0.95 or greater for all the samples of the present system. These features clearly show that the major contribution to the electrical conductivity in the present system may be due to silver ions only.

Conclusions

The present study pertaining to the thermal, structural and electrical characterizations of the mixed system

CuI–Ag_2O–TeO_2 has indicated the formation of silver ion conducting solid electrolytic phases and certain other stable materials containing silver metal as an impurity which may be suitable for widespread applications.

References

1. Takahashi T, Kozawa A (1980) Applications of solid electrolytes. JEC, Ohio
2. Chowdari BVR, Radhakrishna S (1988) Solid state ionic devices. World Scientific, Singapore
3. Takahashi T (1989) High conductivity solid ionic conductors – recent trends and applications. World Scientific, Singapore
4. Laskar AL, Chandra S (1989) Superionic solids and solid electrolytes – recent trends. Academic, San Diego
5. Geller S (1977) Solid electrolytes. Springer, Berlin Heidelberg New York, p 12
6. Minami T (1986) In: Chowdari BVR, Radhakrishna S (eds) Materials for solid state batteries. World Scientific, Singapore, pp 169–179
7. Minami T (1983) J Non-Cryst Solids 56:15
8. Rossignol S, Reau JM, Tanguy B, Videau JJ, Portier J (1993) J Non-Cryst Solids 155:77
9. Suthanthiraraj SA, Mala R (2001) Solid State Ionics 144:143
10. Chandrasekhar VG, Suthanthiraraj SA (1993) J Mater Sci 28:4043
11. Viswanathan A, Suthanthiraraj SA (1992) Solid State Ionics 58:89
12. Viswanathan A, Suthanthiraraj SA (1993) Mater Res Bull 28:821
13. Gogulamurali N, Suthanthiraraj SA, Maruthamuthu P (1996) Solid State Ionics 86–88:1403
14. Suthanthiraraj SA, Murugesan S, Maruthamuthu P (2001) Solid State Ionics 143:413
15. Suthanthiraraj SA, Murugesan S, Maruthamuthu P (2002) Mater Sci Eng B94:207
16. Murugesan S, Suthanthiraraj SA, Maruthamuthu P (2002) Solid State Ionics 148:417
17. Burley G (1963) Am Miner 48:1266
18. Tallan NM, Graham HC, Wimmer JM (1966) Mater Sci Res 3:111
19. Macdonald JR (1974) J Electronal Chem 53:1
20. Macdonald JR (1973) J Chem Phys 58:4982
21. Macdonald JR (1974) J Chem Phys 61:3977
22. Macdonald JR (1987) Impedance spectroscopy. Wiley-Interscience, New York, p 206
23. Wagner JB Jr, Wagner C (1957) J Chem Phys 26:1597
24. Agrawal RC (1999) Indian J Pure Appl Phys 37:294
25. Mckechnie JS, Turner LDS, Vincent CA (1979) J Chem Thermodyn 11:1189
26. Nakamoto K (1997) Infrared and Raman spectra of inorganic and coordination compounds, Part A. Wiley-Interscience, New York, p 223
27. Bentley FF, Smithson LD, Rozek AL (1968) Infrared spectra and characteristic frequencies = 700–300 cm^{-1}. Interscience, New York, p 103